

1 **SKN-1/Nrf2 regulation of neuromuscular function in response to oxidative**  
2 **stress requires EGL-15/FGF Receptor and DAF-2/insulin Receptor signaling in**  
3 ***Caenorhabditis elegans*.**

4  
5 Sungjin Kim\* and Derek Sieburth <sup>\*,†,‡</sup>

6 \*Zilkha Neurogenetic Institute, Keck School of Medicine, University of Southern  
7 California, Los Angeles, California, 90033, USA

8 †Department of Physiology and Neuroscience

9

10

11

12

13

14

15

16

17

18

19

20

21 Running title: RTK signaling in SKN-1 pathway

22 Keywords: SKN-1, neuromuscular junction, oxidative stress, sphingosine kinase

23 ‡corresponding author  
24 Derek Sieburth Ph.D.  
25 Zilkha Neurogenetic Institute  
26 University of Southern California  
27 1501 San Pablo St.  
28 Los Angeles, CA  
29 90033  
30 [sieburth@usc.edu](mailto:sieburth@usc.edu)  
31

32

### 33 **Abstract**

34 The transcription factor Nrf2 plays a critical role in the organism wide-regulation of  
35 the antioxidant stress response. The Nrf2 homolog SKN-1 functions in the intestine  
36 cell non-autonomously to negatively regulate neuromuscular (NMJ) function in  
37 *Caenorhabditis elegans*. To identify additional molecules that mediate SKN-1  
38 signaling to the NMJ, we performed a candidate screen for suppressors of aldicarb-  
39 resistance caused by acute treatment with the SKN-1 activator, arsenite. We  
40 identified two receptor tyrosine kinases, EGL-15 (fibroblast growth factor receptor,  
41 FGFR) and DAF-2 (insulin-like peptide receptor, IR) that are required for NMJ  
42 regulation in response to stress. Through double mutant analysis, we found that  
43 EGL-15 functions downstream of SKN-1 and SPHK-1 (sphingosine kinase), and that  
44 the EGL-15 ligand EGL-17 FGF and canonical EGL-15 effectors are required for  
45 oxidative stress-mediated regulation of NMJ function. DAF-2 also functions  
46 downstream of SKN-1, independently of DAF-16/FOXO, to regulate NMJ function.  
47 Through tissue-specific rescue experiments, we found that FGFR signaling functions

48 primarily in the hypodermis, whereas IR signaling is required in multiple tissues. Our  
49 results support the idea that the regulation of NMJ function by SKN-1 occurs via a  
50 complex organism-wide signaling network involving RTK signaling in multiple  
51 tissues.

52

## 53 **Introduction**

54 The transcription factor Nrf2 plays a crucial role in the maintenance of cellular  
55 redox homeostasis by directing the expression of a cascade of antioxidant, anti-  
56 inflammatory and detoxification enzymes in response to oxidative stress (Blackwell  
57 et al., 2015). In multicellular organisms, Nrf2 activation can confer organism-wide  
58 protection from oxidative stress by regulating stress responses in distal tissues  
59 through inter-tissue signaling. In *C. elegans*, activation of the Nrf2 homolog SKN-1 in  
60 the intestine regulates longevity, survival against xenobiotics and pathogens, and  
61 neurotransmission (Kim and Jin, 2015). Although the cell-autonomous effects of  
62 Nrf2/SKN-1 in promoting cellular survival are well understood, less is known about  
63 how Nrf2/SKN-1 activation leads to changes in oxidative stress responses in distal  
64 tissues.

65 Oxidative stress activates Nrf2/SKN-1 by relieving it from proteolytic  
66 degradation in the cytoplasm and allowing entry into the nucleus where it regulates  
67 gene expression. Nrf2/SKN-1 activity is tightly regulated by phosphorylation and  
68 degradation (Inoue et al., 2005; Leung et al., 2014). Studies in *C. elegans* have  
69 shown that in combination with CUL-4/DDB-1, the ubiquitin ligase WD40 repeat  
70 protein WDR-23 negatively regulates the function of SKN-1 (Choe et al., 2009;

71 Leung et al., 2014). WDR-23 likely dissociates from SKN-1 under conditions in which  
72 oxidative stress is increased, allowing SKN-1 to accumulate in the nucleus (Choe et  
73 al., 2009). SKN-1 activation is regulated by a conserved MAP kinase cascade  
74 composed of NSY-1/MKKK, SEK-1/MKK and PMK-1/MAP kinase, which functions in  
75 the intestine to phosphorylate SKN-1 leading to its stabilization and nuclear  
76 translocation. Once activated, SKN-1 directs the expression of hundreds of genes,  
77 including genes that comprise antioxidant responses such as GST-4, glutathione-S-  
78 transferase.

79 We previously found that SKN-1 activation in the intestine negatively  
80 regulates NMJ function by reducing neuropeptide secretion from motor neurons.  
81 Selective activation of SKN-1 by PMK-1 or by deletion of WDR-23 in the intestine  
82 regulates NMJ function via an inter-tissue signaling mechanism, that involves the  
83 downregulation of sphingosine-1-phosphate production by intestinal SPHK-  
84 1/sphingosine kinase (Kim and Sieburth, 2018b; Staab et al., 2013). Here, we  
85 identify two pathways that function downstream or in parallel of SKN-1 to promote  
86 stress-induced regulation of NMJ function: the fibroblast growth factor receptor  
87 (FGFR) pathway, and the DAF-2 insulin receptor pathway.

88 FGF signaling has well defined functions in animal development, tissue repair  
89 and remodeling. In neurons, FGF signaling regulates synapse formation and  
90 refinement during development. In *C. elegans*, FGF signaling functions in several  
91 developmental processes including cell migration, muscle differentiation, axon  
92 guidance, as well as a post-developmental role in regulating fluid homeostasis  
93 (Bulow et al., 2004; Diaz-Balzac et al., 2015; Huang and Stern, 2004; Lo et al., 2008;  
94 Szewczyk and Jacobson, 2003). The FGF receptor, EGL-15 is activated by one of

95 two FGFs, EGL-17 and LET-756. EGL-15 activates a downstream signaling cascade  
96 composed of the SEM-5/GRB2 adaptor protein, the SOS-1/guanine nucleotide  
97 exchange factor, the SOC-2/SHOC2 adaptor protein and SOC-1, a putative adaptor  
98 with a conserved PHD domain that interacts with SEM-5 (Schutzman et al., 2001).

99 DAF-2 is a subfamily of receptor tyrosine kinase, ortholog of insulin/IGF-1  
100 transmembrane receptor (IR) playing a key regulator of lifespan, stress resistance,  
101 metabolism and development (Gottlieb and Ruvkun, 1994; Hung et al., 2014; Libina  
102 et al., 2003). Neuronal functions of DAF-2 include motor activity, isothermal tracking,  
103 development of cholinergic axon and touch receptor neuron (Duhon and Johnson,  
104 1995; Hsu et al., 2009; Li et al., 2016; Murakami et al., 2005). DAF-2 also plays a  
105 role in the long term and short term learning memory (Kauffman et al., 2010).

106 In this study, we found that the FGF pathway consisting of EGL-17, EGL-15,  
107 SOS-1, SOC-1 and SOC-2 functions downstream of SKN-1 and SPHK-1 to  
108 negatively regulate NMJ function in response to oxidative stress. Surprisingly, EGL-  
109 15 functions primarily in the skin to regulate NMJ function. We found that DAF-2  
110 signaling functions downstream of SKN-1 independently of DAF-16 to regulate NMJ  
111 function. Finally, we showed that DAF-2 may function in multiple distinct tissues to  
112 regulate NMJ function. These results suggest that RTK signaling in multiple tissues  
113 regulates NMJ function in response to oxidative stress.

114

## 115 **Material and methods**

### 116 ***C. elegans* strains**

117 All strains used in this study were maintained at 22°C following standard methods.

118 For temperature sensitive mutants, we transferred L4 stage worms, which were  
119 grown on 22°C, to 25°C for 24 hours prior to assay. Young adult hermaphrodites  
120 were used for all experiments. The following mutant strains were used. Some of  
121 which were provided by the Caenorhabditis Genetics Center, which is funded by NIH  
122 Office of Research Infrastructure Programs (P40 OD010440): *egl-15(n1477ts)*, *egl-*  
123 *15(n484ts)*, *egl-17(ay6)*, *let-756(s2163)*, *sos-1(cs41ts)*, *soc-1(n1789)*, *soc-2(n1774)*,  
124 *sem-5(n1799)*, *daf-2(e1370ts)*, *daf-2(m596ts)*, *daf-16(mu86)*, ZM8561 [*daf-*  
125 *2(m596);hpEx2906(Pmyo-2::RFP + Prgef-1::daf-2)*], ZM8562 [*daf-*  
126 *2(m596);hpEx2369(Pmyo-2::RFP + Pges-1::daf-2)*], ZM8988 [*daf-*  
127 *2(m596);hpEx2908(Pmyo-2::RFP + Pdpy-30::daf-2)*], ZM9028 [*daf-*  
128 *2(m596);hpEx2905(Pmyo-2::RFP + Pmyo-3::daf-2)*], NH2447 [*ayls2(egl-15p::GFP +*  
129 *dpy-20(+)*]. The *wdr-23(tm1718)* strain was provided by National BioResource  
130 Project (Japan). The wild type reference strain was N2 Bristol. The genes and  
131 mutant strains tested in our screen are listed in the Supplemental file 1.

### 132 **Molecular biology**

133 All genes were cloned from *C. elegans* cDNA or genomic DNA from wild type worms  
134 and inserted into pPD49.26 using standard molecular biology techniques. Promoter  
135 DNA fragments were amplified from mixed stage genomic DNA. The following  
136 plasmids were generated and used: *pSK46[Pges-1::egl-15(genomic)]*, *pSK47[Prab-*  
137 *3::egl-15(genomic)]*, *pSK48[Pcol-12::egl-15(genomic)]*, *pSK57[Pcol-12::daf-*  
138 *2(genomic)]*, *pSK80[Pegl-15::gfp]*.

### 139 **Transgenic lines**

140 Transgenic strains were generated by injecting expression constructs (10–25 ng/μl)

141 and the coinjection marker KP#708 (*Pttx-3::rfp*, 40 ng/μl) or KP#1106 (*Pmyo-2::gfp*  
142 10 ng/μl) into N2 or corresponding mutants. Microinjection was performed following  
143 standard techniques as previously described (Mello et al., 1991). At least three lines  
144 for each transgene were tested and a representative transgene was used for the  
145 further experiments. The following transgenic arrays were made: *vjEx1309[Pcol-*  
146 *12::daf-2]*, *vjEx1239[Prab-3::egl-15]*, *vjEx1241[Pges-1::egl-15]*, *vjEx1243[Pcol-*  
147 *12::egl-15]*, *vjEx1593[Pegl-15::gfp]*.

### 148 **Microscopy and analysis**

149 Fluorescence microscopy experiments were performed following previous methods  
150 (Kim and Sieburth, 2018a). Briefly, for all fluorescence microscopy analysis, L4 stage  
151 or young adult worms were immobilized by using 2,3-butanedione monoxime (BDM,  
152 30 mg/mL; Sigma) in M9 buffer then mounted on 2% agarose pads for imaging. To  
153 image and quantify the intestinal fluorescence intensity of *Pgst-4::GFP* and *Pegl-*  
154 *15::GFP* posterior intestinal cells were selected as a representative region. Images  
155 were captured with the Nikon eclipse 90i microscope equipped with a Nikon PlanApo  
156 40 x or 60x or 100x objective (NA = 1.4) and a PhotometricsCoolsnap ES2 or a  
157 Hamamatsu Orca Flash LT+ CMOS camera. Metamorph 7.0 software (Universal  
158 Imaging/Molecular Devices) was used to capture serial image stacks, and the  
159 maximum intensity was measured (Kim and Sieburth, 2018a). Intensity quantification  
160 analysis was performed on the same day to equalize the absolute fluorescence  
161 levels between samples within same experimental set.

### 162 **RNA Interference**

163 Feeding RNAi knockdown assay was performed following the established protocol

164 (Kamath and Ahringer, 2003). Briefly, gravid adult animals were placed on RNAi  
165 plates seeded with HT115(DE3) bacteria transformed with L4440 vector containing  
166 fragment of knockdown genes or empty L4440 vector as a control to collect eggs  
167 then removed after 4 hours to obtain age-matched synchronized worm population.  
168 Young adult animals were used for every RNAi assay.

## 169 **Pharmacology**

170 For aldicarb assays, the percentage of paralyzed young adult animals was counted  
171 every 10 to 15 minutes starting about one hour after placing worms on 1mM aldicarb  
172 (Bayer) plates. NGM Plates containing aldicarb were freshly made one day before  
173 each assay. Wild type animals were included in each set of assays to control for  
174 assay-to-assay variability arising from slightly different aldicarb concentrations in  
175 each batch of assay plates. Two to three replicates of at least 20 worms were  
176 performed per strain analyzed. For arsenite exposure, at least 50 young adult  
177 animals were transferred to NGM plates supplemented with 5mM sodium arsenite  
178 (RICCA Chemicals) for 4 hours prior to aldicarb assay and *Pegl-15::gfp* imaging. To  
179 induce arsenite-activated *Pgst-4::gfp*, at least 50 young adult animals were  
180 incubated with 5mM arsenite in M9 buffer for 1 hour, then images were taken after 4  
181 hours of recovery.

## 182 **Statistical Analysis**

183 For the Figure 1D and E, the Student's t test (two-tailed) was used to determine the  
184 statistical significance. "ns" above the bars denotes P values greater than 0.05. Error  
185 bars in the figures indicate  $\pm$ SEM. The numbers of animals tested are indicated in  
186 each figure.



## 187 **Data Availability**

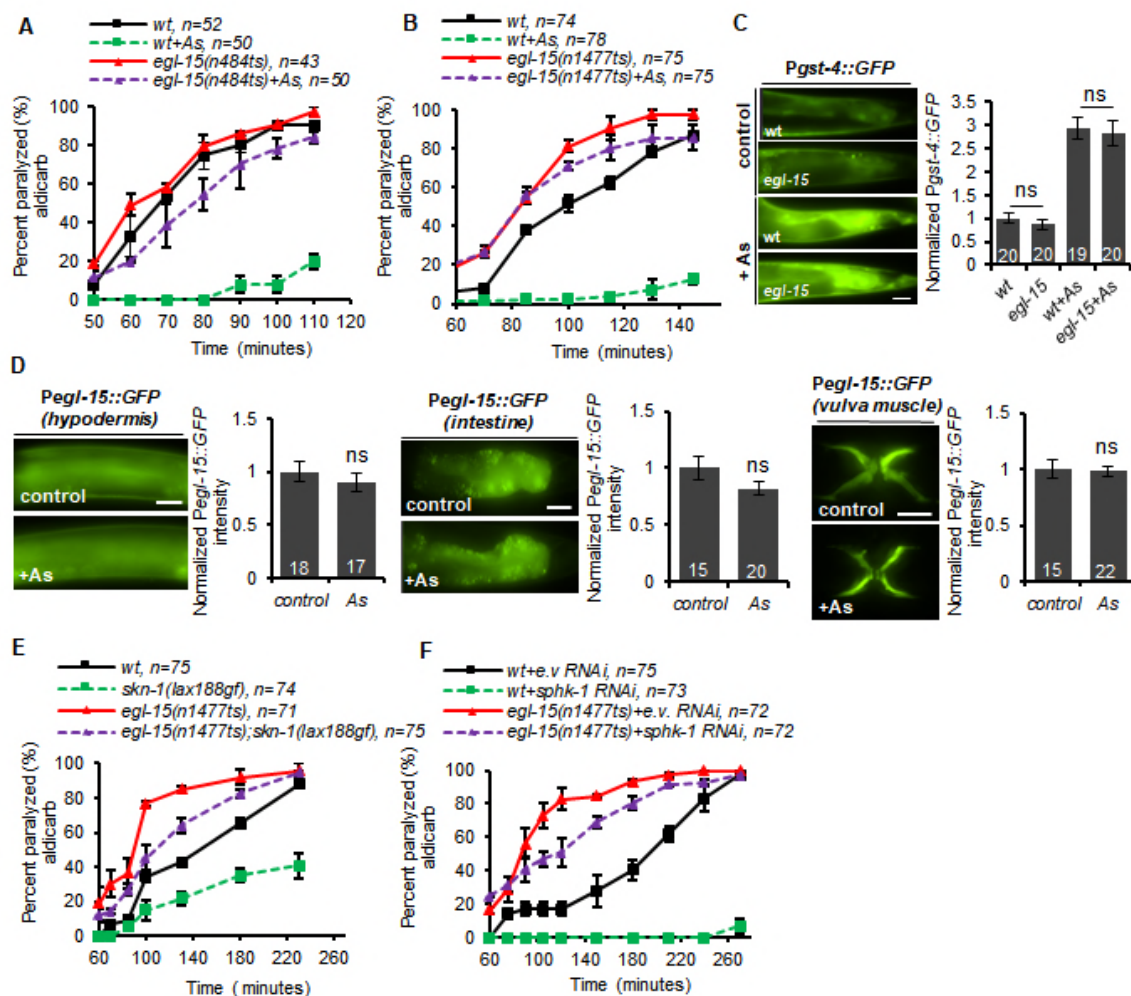
188 Strains and plasmids used in this study are available upon request. The authors  
189 clarify that all data necessary for confirming the conclusions of the findings are  
190 present within the article, figures, and supplemental file.

## 191 **Results**

### 192 **A screen for genes that promote aldicarb resistance in response to oxidative** 193 **stress.**

194 We previously showed that acute (4 hour) exposure to the oxidative stressor  
195 arsenite causes resistance to the paralytic effects of aldicarb (Kim and Sieburth,  
196 2018b; Staab et al., 2013). Aldicarb is an acetylcholine esterase inhibitor, and  
197 aldicarb treatment leads to acetylcholine accumulation in synaptic clefts at  
198 neuromuscular junctions and subsequent paralysis due to muscle hyper-contraction.  
199 Animals defective in acetylcholine secretion exhibit delayed paralysis (referred to  
200 here as aldicarb resistance) because of a delay in acetylcholine accumulation in  
201 synaptic clefts. Arsenite causes aldicarb resistance by activating the SKN-1 pathway  
202 in the intestine (Kim and Sieburth, 2018b; Staab et al., 2013). To identify additional  
203 genes that mediate the effects of arsenite on neuromuscular function, we performed  
204 a large-scale candidate screen for mutants that blocked or attenuated aldicarb  
205 resistance caused by arsenite treatment. We selected 90 candidate genes based on  
206 their known roles in presynaptic function, signaling transduction, protein secretion, or  
207 stress response (Supplemental file 1). Nearly all of the mutants corresponding to  
208 these genes had wild type responses to arsenite, with the exception of *sphk-1*, *pmk-*  
209 *1*, *sek-1* and *nsy-1* mutants, which were included as positive controls, as well as two

210 additional mutants: *egl-15*/FGFR and *daf-2*/IGFR. Both *egl-15* and *daf-2* mutants  
 211 significantly attenuated the ability of arsenite treatment to cause aldicarb resistance  
 212 (Supplemental file 1), revealing a potential role for FGF and IR signaling in regulating  
 213 stress-induced aldicarb response.  
 214



215

216 **Figure 1. EGL-15 functions downstream of SKN-1 and SPHK-1 to promote arsenite-**  
 217 **induced aldicarb resistance.** (A-B) Time course of aldicarb-induced paralysis of wild type  
 218 (wt) or *egl-15* (n1477ts) or *egl-15* (n484ts) mutants following arsenite treatment (As). (C)  
 219 Representative images of posterior intestines of indicated strains expressing GFP driven

220 under the *gst-4* promoter (*left*) in the absence or presence of arsenite (As). Quantification of  
221 the average GFP intensity (*right*). (D) Representative images and quantification of GFP  
222 driven under *egl-15* promoter in hypodermis (*upper left*), intestine (*upper right*) and vulva  
223 muscle (lower) following control or arsenite treatment. (E) Time course of aldicarb-induced  
224 paralysis of wild type control, *skn-1(lax188 gain-of-function)*, *egl-15(n1477ts)* or *skn-*  
225 *1(lax188gf);egl-15* double mutants. (F) Time course of aldicarb-induced paralysis of wild type  
226 (wt) and *egl-15* mutants treated with empty vector (e.v.) control or *sphk-1* RNAi. “ns” above  
227 the bars denotes P values greater than 0.05. Number of animals tested are indicated. Error  
228 bars indicate  $\pm$ SEM.

229

### 230 **EGL-15 promotes arsenite-induced aldicarb resistance.**

231 *egl-15* encodes the sole *C. elegans* ortholog of the fibroblast growth factor  
232 receptor (FGFR). Temperature sensitive *egl-15* mutants are viable at the permissive  
233 temperature (22°C) and display a scrawny phenotype when grown at the restrictive  
234 temperature of 25°C (Dixon et al., 2006). *egl-15(n484ts)* mutants, which encode a  
235 W167Stop nonsense mutation, were shifted to 25°C as L4s, when development is  
236 complete, and assayed for aldicarb responsiveness as adults, 24 hours later. We  
237 found that the shifted *egl-15(n484ts)* mutants exhibited similar aldicarb sensitivity as  
238 wild type controls in the absence of arsenite. However, *egl-15(n484ts)* mutants  
239 became significantly less aldicarb resistant than wild type controls following arsenite  
240 treatment (Figure 1A). A second temperature sensitive *egl-15* mutant, (*n1477ts*),  
241 which encodes a W930Stop nonsense mutation (DeVore et al., 1995), exhibited  
242 slight but significant hypersensitivity to aldicarb following temperature up-shift  
243 compared to wild type controls in the absence of arsenite (Figure 1B). In the  
244 presence of arsenite, *egl-15(n1477ts)* mutants remained nearly as aldicarb  
245 hypersensitive as untreated mutants (Figure 1B). Thus, EGL-15 has a post-  
246 developmental role in promoting arsenite-induced aldicarb resistance.

### 247 **EGL-15 functions downstream of SKN-1 and SPHK-1 to promote arsenite-**

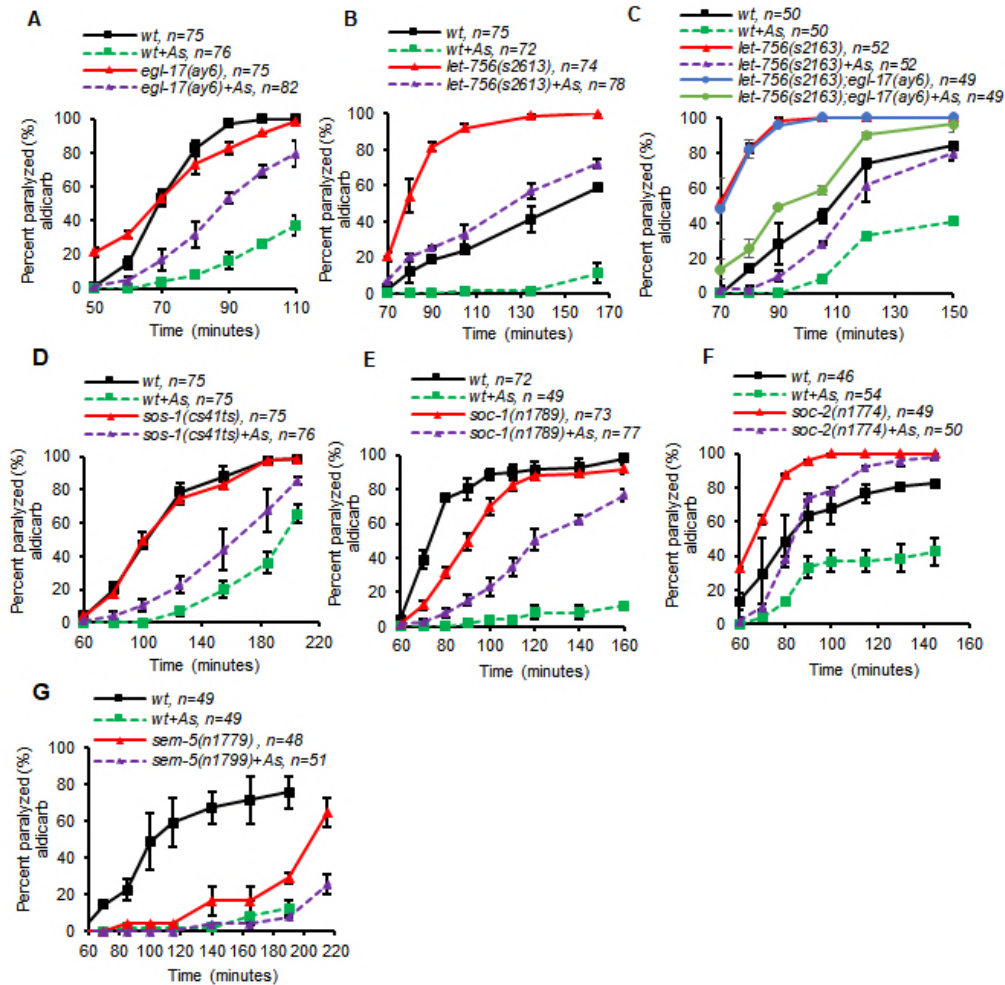
248 **induced aldicarb resistance.**

249 To determine whether EGL-15 is a SKN-1 activator, we examined the  
250 requirement of *egl-15* in the stress-induced expression of *gst-4*/glutathione-S-  
251 transferase, which is a direct transcriptional target of SKN-1 (Choe et al., 2009; Wu  
252 et al., 2016). A transcriptional reporter in which GFP is expressed under the *gst-4*  
253 promoter (*Pgst-4::GFP*) is expressed at low levels in the absence of stress whereas  
254 arsenite treatment significantly increases *Pgst-4::GFP* expression in the intestine in a  
255 *skn-1*-dependent manner (Choe et al., 2009; Wu et al., 2016). We found that the  
256 expression of *Pgst-4::GFP* in the intestine was similar in *egl-15* mutants and wild  
257 type controls in the absence of arsenite (Figure 1C). Following four hour arsenite  
258 treatment, *Pgst-4::GFP* expression increased about three-fold in wild type controls,  
259 and we observed a similar three-fold increase in *egl-15* mutants (Figure 1C). Thus,  
260 both baseline SKN-1 activity and arsenite-induced activation of SKN-1 are normal in  
261 *egl-15* mutants, suggesting that EGL-15 does not regulate SKN-1 activity.

262 To determine whether EGL-15 is a transcriptional target of SKN-1, we  
263 examined the effects of arsenite treatment on the fluorescence intensity of *Pegl-15::GFP*  
264 reporters, in which the 2.0 kb promoter fragment of *egl-15* drives the  
265 expression of GFP. We found that transgenic animals expressing *Pegl-15::GFP*  
266 exhibited fluorescence in the intestine, vulval muscle and hypodermis, in agreement  
267 with prior studies (Bulow et al., 2004; Mounsey et al., 2002). Arsenite treatment did  
268 not significantly alter the fluorescence intensity of *Pegl-15::GFP* in any of these  
269 tissues (Figure 1D). These results suggest that EGL-15 is not transcriptionally  
270 regulated by SKN-1 activation.

271 To determine whether EGL-15 functions in the SKN-1 pathway to regulate  
272 aldicarb resistance, we examined *skn-1* mutants that are constitutively active. The  
273 *skn-1(lax188gf)* mutation alters an amino acid in a protein-interaction domain that  
274 renders SKN-1 constitutively active (Paek et al., 2012). *skn-1(lax188gf)* mutants are  
275 aldicarb resistant (Staab et al., 2013). We found that *egl-15* mutations significantly  
276 reduced the aldicarb resistance of *skn-1(lax188gf)* mutants (Figure 1E). SKN-1  
277 activation leads to aldicarb resistance in part by negatively regulating SPHK-1  
278 signaling in the intestine (Kim and Sieburth, 2018b). To determine whether EGL-15  
279 mediates the effects of SPHK-1 in this pathway, we examined aldicarb responses of  
280 *egl-15* mutants where intestinal *sphk-1* activity is knocked down by RNAi. Animals  
281 treated with *sphk-1* RNAi are strongly resistant to aldicarb (Chan et al., 2012; Kim  
282 and Sieburth, 2018b). Strikingly, *egl-15* mutations nearly completely suppressed the  
283 aldicarb resistance caused by *sphk-1* RNAi (Figure 1F). These results indicate that  
284 EGL-15 and SPHK-1 function antagonistically to regulate aldicarb responsiveness,  
285 and that EGL-15 functions downstream of or in parallel to SPHK-1. Together, these  
286 results reveal a role for EGL-15 in regulating neuromuscular function in response to  
287 SKN-1 activation.

288



289

290 **Figure 2. EGL-17 FGF and the SOS-1/SOC-1/SOC-2 signaling cascade is required for**  
 291 **arsenite-induced aldicarb resistance.** (A-G) Time course of aldicarb-induced paralysis of  
 292 indicated strains in the absence or presence of arsenite. Number of animals tested are  
 293 indicated. Error bars indicate  $\pm$ SEM.

294

295 **The FGF ligand EGL-17 mediates arsenite-induced aldicarb resistance.**

296 Two FGF-related ligands signal through EGL-15 to control distinct functions of  
 297 EGL-15. EGL-17/FGF promotes sex myoblast migration while LET-756/FGF  
 298 promotes axon guidance and fluid homeostasis (Birnbaum et al., 2005; Burdine et  
 299 al., 1997; DeVore et al., 1995; Diaz-Balzac et al., 2015; Lo et al., 2008; Popovici et  
 300 al., 1999; Sundaram et al., 1996). To determine whether either of these FGF ligands

301 promotes stress-induced aldicarb resistance, we examined aldicarb responses of  
302 *egl-17* and *let-756* mutants. *egl-17(ay6)* is a deletion allele that is predicted to  
303 eliminate *egl-17* activity (Burdine et al., 1997). *egl-17(ay6)* mutants displayed wild  
304 type aldicarb responsiveness in the absence of arsenite. Following arsenite  
305 treatment, *egl-17(ay6)* mutants became more aldicarb resistant than untreated  
306 mutants, but this shift in aldicarb resistance was significantly smaller than that of wild  
307 type controls treated with arsenite (Figure 2A). This partial response suggests that  
308 EGL-17 contributes to arsenite-induced aldicarb resistance, but is not likely to be  
309 solely responsible for EGL-15 activation in this process.

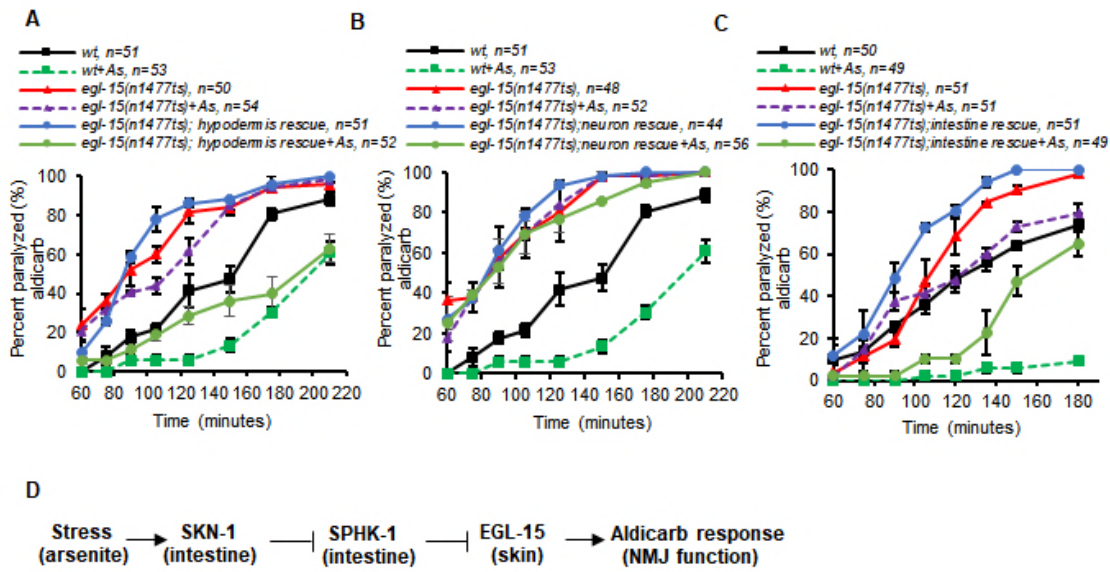
310 To test the role of LET-765, we examined *let-756(s2613)* hypomorphic  
311 mutants, which are viable, unlike null mutants, which die as larvae (Popovici et al.,  
312 2004). *let-756(s2613)* mutants were significantly more sensitive to aldicarb-induced  
313 paralysis than wild type controls in the absence of arsenite (Figure 2B), revealing a  
314 role for LET-765 in inhibiting NMJ function in the absence of stress. Arsenite  
315 treatment caused a large shift toward aldicarb resistance in *let-756* mutants that was  
316 similar to that of wild type controls (Figure 2B), suggesting that stress-induced  
317 aldicarb resistance is not impaired in these mutants. The partial defect in arsenite-  
318 induced aldicarb resistance of *egl-17* mutants was not enhanced by *let-756*  
319 mutations (Figure 2C). Thus, we conclude that EGL-17 contributes to arsenite-  
320 induced aldicarb resistance, and LET-756 may not. However, because the *let-756*  
321 mutant analyzed was not null, it is not possible to make a definitive determination of  
322 its contribution in this pathway.

323

324 **The SOS-1/SOC-1/SOC-2 signaling cascade mediates arsenite-induced**  
325 **aldicarb resistance.**

326 We next examined mutants corresponding to each of the known components  
327 that make up the signaling cascade downstream of EGL-15 for defects in arsenite-  
328 induced aldicarb resistance. *sos-1(cs41ts)* mutants are temperature sensitive  
329 (Abdus-Saboor et al., 2011), and when shifted to 25°C for 24 hours prior to assay,  
330 exhibited wild type aldicarb responsiveness in the absence of stress. *sos-1(cs41ts)*  
331 mutants became significantly less aldicarb resistant following arsenite treatment than  
332 wild type controls (Figure 2D). *soc-1(n1789)* and *soc-2 (n1774)* are null and  
333 hypomorph alleles, respectively (Schutzman et al., 2001). We found that *soc-*  
334 *1(n1789)* mutants were slightly aldicarb resistant in the absence of arsenite whereas  
335 *soc-2 (n1774)* mutants were hypersensitive to aldicarb (Figure 2E, F). However, both  
336 mutants became significantly less aldicarb resistant than wild type controls following  
337 arsenite treatment (Figure 2E, F). Finally, *sem-5(n1779)* hypomorphic mutants were  
338 extremely resistant to aldicarb in the absence of arsenite, revealing a role of SEM-5  
339 promoting NMJ function. Arsenite treatment elicited a further increase in aldicarb  
340 resistance in *sem-5(n1779)* mutants, but this shift was much smaller than the shift  
341 elicited in wild type controls (Figure 2G). Thus, SOS-1, SOC-1 and SOC-2 contribute  
342 to stress-induced aldicarb resistance. The contribution of SEM-5 is more difficult to  
343 ascertain given that the mutants were so resistance to aldicarb in the absence of  
344 stress. Because EGL-15 signaling is left partially intact in each of the signaling  
345 mutants tested, we conclude that these components may function in parallel with  
346 each other, or may function with other unidentified components activated by EGL-15  
347 to contribute to stress-induced aldicarb responsiveness.





348

349 **Figure 3. EGL-15 is required in the hypodermis to regulate arsenite mediated aldicarb**  
 350 **resistance.** (A-C) Time course of aldicarb-induced paralysis of the indicated strains in the  
 351 absence or presence of arsenite (As). “hypodermis rescue, neuron rescue, intestine rescue,”  
 352 denotes *egl-15* transgene expression using the tissue-specific promoters *col-12*, *rab-3*, or  
 353 *ges-1*, respectively. (D) Schematic working model whereby EGL-15 signaling in the skin (and  
 354 intestine) is negatively regulated by SPHK-1 signaling in the intestine during low stress  
 355 conditions. Following SKN-1 activation by oxidative stress, SPHK-1 activity is inhibited,  
 356 which in turn leads to increased EGL-15 activity resulting in aldicarb resistance. Number of  
 357 animals tested are indicated. Error bars indicate  $\pm$ SEM.

358

359 **EGL-15 functions in the hypodermis to promote arsenite-induced aldicarb**  
 360 **resistance.**

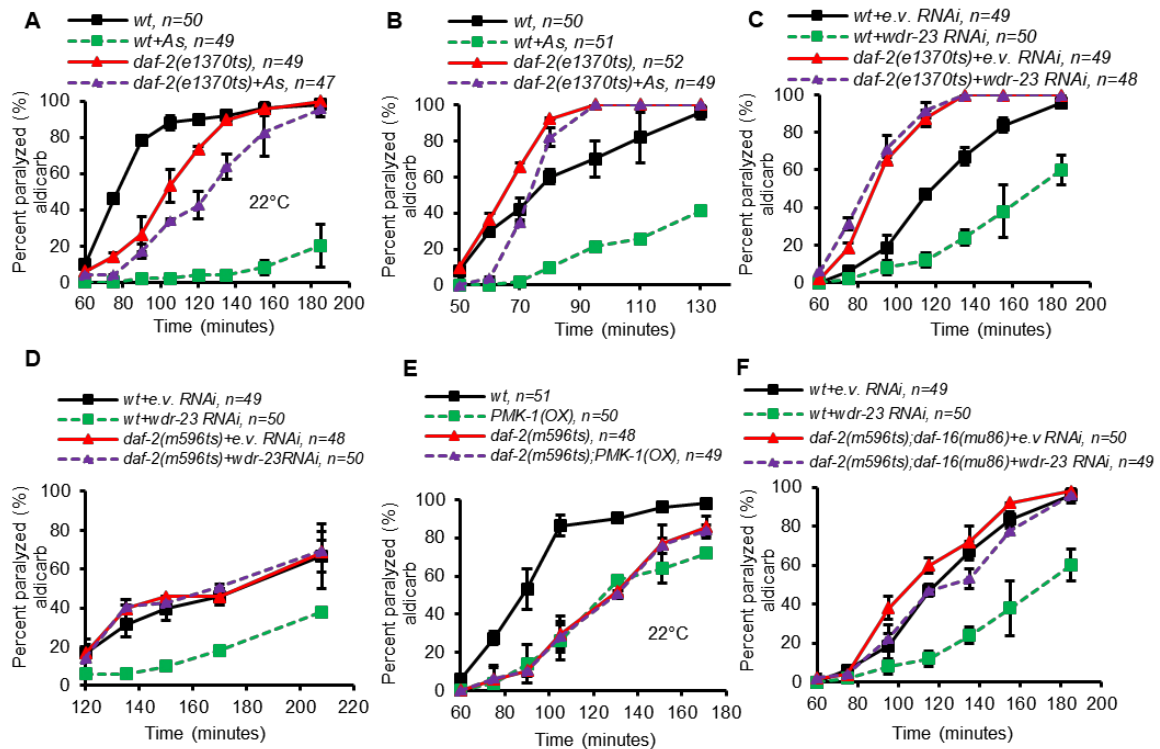
361 EGL-15 has been reported to be expressed in multiple tissues, including the  
 362 hypodermis, vulval muscles, intestine and neurons (Bulow et al., 2004; Huang and  
 363 Stern, 2004). To determine the site of action of EGL-15 with respect to stress-  
 364 induced aldicarb resistance, we performed tissue-specific rescue experiments by  
 365 generating transgenic *egl-15(n1477ts)* mutants expressing *egl-15* genomic DNA  
 366 selectively in the hypodermis (using the *col-12* promoter (Olofsson, 2014)), intestine

367 (using the *ges-1* promoter(Kim and Sieburth, 2018a)) or nervous system (using the  
368 *rab-3* promoter (Kim and Sieburth, 2018b)). Expression of *egl-15* in each of these  
369 tissues did not rescue the weak aldicarb hypersensitivity of *egl-15(n1477ts)* mutants  
370 in the absence of stress, suggesting that the basal response of *egl-15(n1477ts)*  
371 mutants to aldicarb may require EGL-15 signaling in multiple tissues or in other  
372 tissue(s) not tested here (Figure 3A-C). However, EGL-15 expression in the  
373 hypodermis fully restored arsenite-induced aldicarb resistance to *egl-15(n1477ts)*  
374 mutants (Figure 3A). In contrast, expression of *egl-15* transgenes in the nervous  
375 system failed to rescue the aldicarb sensitivity of *egl-15(n1477ts)* mutants (Figure  
376 3B), and expression of *egl-15* in the intestine partially restored stress-induced  
377 aldicarb resistance to *egl-15(n1477ts)* mutants (Figure 3C). These results suggest  
378 that EGL-15 signaling in the hypodermis is critical for arsenite-induced aldicarb  
379 resistance. Our results support a model whereby under conditions of low stress,  
380 EGL-15 signaling is inhibited by SPHK-1 in the intestine. During stress, SPHK-1  
381 activity is inhibited by SKN-1 activation, which in turn leads to increased EGL-15  
382 signaling in the skin (and possibly also the intestine) and negative regulation of  
383 neuromuscular function (Figure 3D).

384

385

386



387

388 **Figure 4. DAF-2 functions downstream of SKN-1 to regulate NMJ function.** (A-B) Time  
 389 course of aldicarb-induced paralysis of wild type control (wt) and *daf-2(e1370ts)* mutants  
 390 grown at 22°C (A) or 25°C for 24 hours (B) prior to aldicarb assays following control or  
 391 arsenite treatment. (C-D) Time course of aldicarb-induced paralysis of indicated strains  
 392 treated with empty vector (e.v.) control or *wdr-23* RNAi. (E) Time course of aldicarb-induced  
 393 paralysis of indicated strains. *PMK-1(OX)* denotes animals over-expressing *pmk-1*  
 394 transgenes in the intestine. (F) Time course of aldicarb-induced paralysis of indicated strains  
 395 following empty vector (e.v.) control or *wdr-23* RNAi treatment. Number of animals tested are  
 396 indicated. Error bars indicate  $\pm$ SEM.

397

### 398 **DAF-2 is required for aldicarb resistance induced by oxidative stress.**

399 The second gene identified in our screen was *daf-2*. We examined two  
 400 temperature sensitive *daf-2* mutants, *daf-2(e1370ts)*, which encodes a P1547S  
 401 missense mutation, and *daf-2(m596ts)*, which encodes a G471S missense mutation  
 402 (Bulger et al., 2017). Both mutants are viable at the semi-permissive temperature of

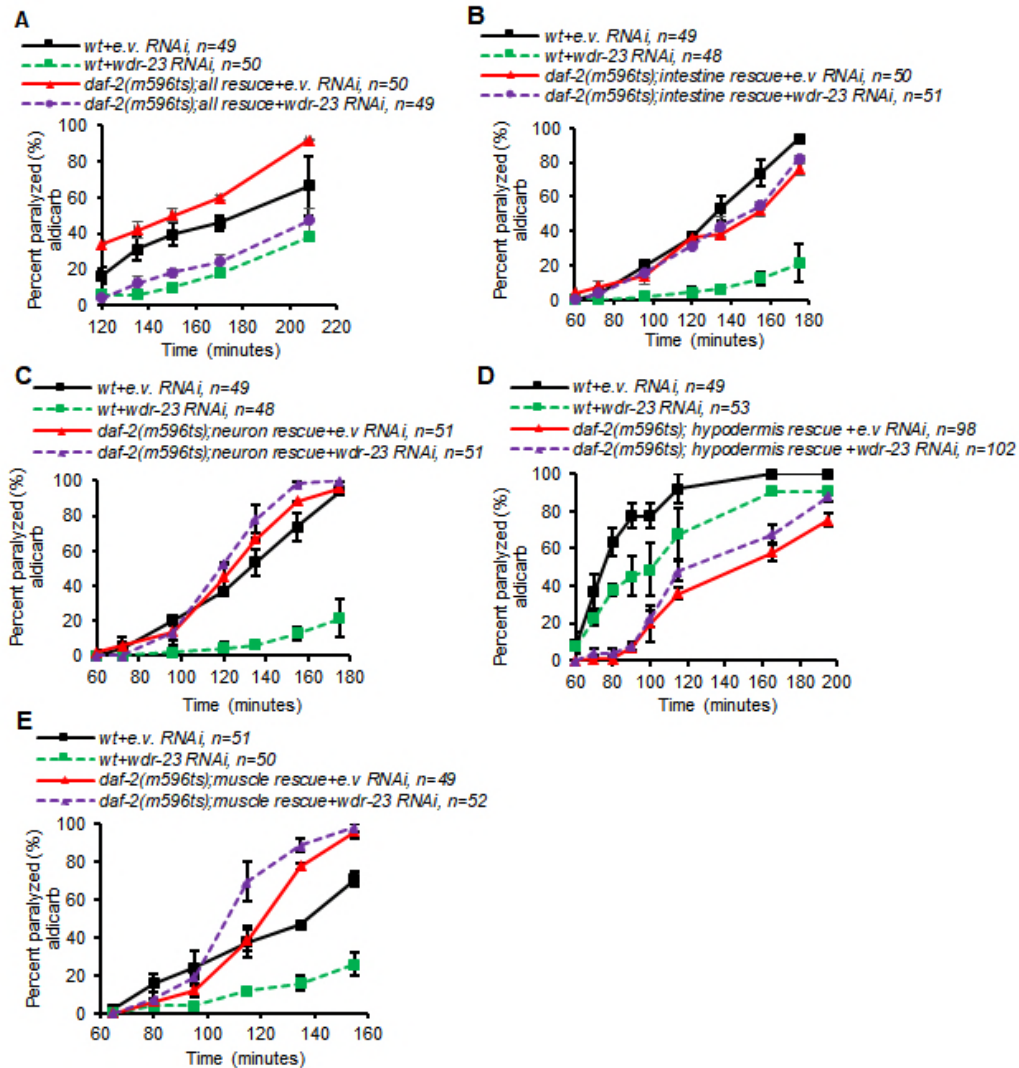
403 22°C and enter into the dauer stage at the restrictive temperature of 25°C (Bulger et  
404 al., 2017). In the absence of arsenite, both *daf-2(e1370ts)* and *daf-2(m596ts)*  
405 mutants were slightly more aldicarb resistant than wild type controls when cultured at  
406 22°C (Figure 4A and 4E). Following arsenite treatment, *daf-2(e1370ts)* mutants  
407 failed to become more aldicarb resistant than untreated mutants, remaining nearly as  
408 sensitive to aldicarb as untreated *daf-2* controls (Figure 4A). These results reveal a  
409 role for DAF-2 in promoting arsenite-induced aldicarb resistance in adult animals that  
410 is distinct from its role in regulating development.

#### 411 **DAF-2 functions downstream or in parallel to SKN-1**

412 To determine whether DAF-2 functions in the SKN-1 pathway to regulate  
413 aldicarb responsiveness, we examined the aldicarb responsiveness of *daf-2* mutants  
414 in which SKN-1 is constitutively active. WDR-23 promotes neuromuscular function by  
415 negatively regulating SKN-1 in the intestine. *wdr-23* null mutants show delayed  
416 aldicarb paralysis in the absence of stress that is completely dependent upon *skn-1*  
417 and is not enhanced by arsenite treatment (Kim and Sieburth, 2018b; Staab et al.,  
418 2013). As expected, *wdr-23* knockdown by RNAi led to strong aldicarb resistance.  
419 However, knockdown of *wdr-23* was unable to cause aldicarb resistance in either  
420 *daf-2(e1370ts)* or *daf-2(m596ts)* mutants (Figure 4C, D), suggesting that the aldicarb  
421 resistance phenotype caused by SKN-1 activation is dependent upon *daf-2*  
422 signaling. PMK-1 positively regulates SKN-1 activity in the intestine by  
423 phosphorylating SKN-1, leading to its stabilization and its accumulation in the  
424 nucleus (Inoue et al., 2005). Animals over-expressing PMK-1 cDNA specifically in  
425 intestine (under the *ges-1* promoter) exhibited enhanced aldicarb resistance  
426 compared to non-transgenic controls (Figure 4E and (Kim and Sieburth, 2018b)).

427 However, PMK-1 overexpression was unable to make *daf-2(m596ts)* mutants more  
428 aldicarb resistant than non-transgenic controls (Figure 4E). Together, these results  
429 are consistent with a function of DAF-2 either downstream or in parallel to SKN-1 in  
430 regulating aldicarb resistance in response to stress.

431 DAF-2 signaling exerts its biological effects by either negatively regulating the  
432 DAF-16/FOXO transcription factor (Chen et al., 2013; Simon et al., 2014; Sun et al.,  
433 2017)), or by a mechanism that is independent of DAF-16 (Szewczyk et al., 2007). If  
434 DAF-2 negatively regulates DAF-16 in this stress response, we predict that *daf-16*  
435 mutations should restore SKN-1-induced aldicarb resistance to *daf-2* mutants. We  
436 found that *daf-2; daf-16* double mutants exhibited aldicarb responsiveness that was  
437 similar to *daf-2* single mutants (Figure 4F). However, *daf-16* mutations did not  
438 restore aldicarb resistance to *daf-2* mutants treated with *wdr-23* RNAi (Figure 4D and  
439 4F). This result suggests that DAF-2-mediated regulation of aldicarb resistance does  
440 not require DAF-16 signaling.



441

442 **Figure 5. DAF-2 functions in multiple tissues to regulate SKN-1 dependent NMJ**  
 443 **function.** (A-E) Time course of aldicarb-induced paralysis of wild type (wt) animals or *daf-*  
 444 *2(m596ts)* transgenic mutants following empty control (e.v.) or *wdr-23* RNAi treatment. “all  
 445 rescue, intestine rescue, neuron rescue, hypodermis rescue, muscle rescue” denotes DAF-2  
 446 transgenes expressing under the tissue-specific promoters *dyp-30*, *ges-1*, *rab-3*, *col-12* or  
 447 *myo-3*, respectively. Number of animals tested are indicated. Error bars indicate  $\pm$ SEM.

448

449

450

451 **DAF-2 functions in multiple tissues to promote arsenite-induced aldicarb**  
452 **resistance**

453 DAF-2 is expressed in multiple tissues including intestine, nervous system,  
454 hypodermis and muscle (Hunt-Newbury et al., 2007; McKay et al., 2003). To identify  
455 the tissue in which DAF-2 functions in SKN-1-mediated aldicarb resistance, we  
456 performed a series of tissue-specific rescue experiments using *daf-2* genomic DNA.  
457 A prior study generated a panel of extrachromosomal arrays in which *daf-2* genomic  
458 DNA was expressed in different tissues (Hung et al., 2014). We examined strains  
459 bearing these extrachromosomal arrays for their ability to restore normal stress-  
460 induced aldicarb resistance to *daf-2(m596ts)* mutants. To activate the stress  
461 response, we knocked down *wdr-23* by RNAi in *daf-2(m596ts)* mutants. As  
462 expected, expression of *daf-2* genomic DNA in all tissues (using the *dpy-30*  
463 promoter) fully reverted aldicarb resistance to *daf-2* mutants treated with *wdr-32*  
464 RNAi (Figure 5A). Next, we tested whether DAF-2 expression selectively in the  
465 intestine (using the *ges-1* promoter), the nervous system (using the *rab-3* promoter),  
466 the hypodermis (using the *col-12* promoter), or in body wall muscle (using the *myo-3*  
467 promoter) could restore normal aldicarb responsiveness to *daf-2(m596ts)* mutants in  
468 which *wdr-23* was knocked down. Interestingly, we found that expression of DAF-2 in  
469 any single tissue failed to rescue *daf-2(m596ts)* mutants (Figure 5B-E). These  
470 results suggest that DAF-2 may function in more than one tissue to regulate SKN-1  
471 mediated aldicarb resistance. Alternatively, DAF-2 may function in a tissue not tested  
472 here, such as the germ line to regulate aldicarb responsiveness.

473

## 474 **Discussion**

475           Multicellular organisms are exposed to variety of stresses in the form of  
476 endogenous or environmental stress-induced by changes in their surroundings.  
477 Therefore, they have developed complex organism-wide defense mechanism to  
478 prevent the cellular damage and maintain proper cellular homeostasis. Our results  
479 support the idea that the regulation of NMJ function by oxidative stress is mediated  
480 by complex signaling networks that act across multiple tissues and involve at least  
481 two RTK signaling cascades, FGFR and IR. Our genetic analysis revealed that both  
482 of these RTKs likely function downstream of SKN-1 to promote aldicarb resistance  
483 caused by acute oxidative stress. Our temperature shift experiments show that these  
484 RTK pathways regulate NMJ physiology rather than development. We found that  
485 EGL-15 functions primarily in the hypodermis to regulate NMJ function, whereas  
486 DAF-2 signaling may be required in multiple different tissues. Thus, EGL-15 and  
487 DAF-2 signaling may mediate inter-tissue communication between the intestine,  
488 where SKN-1 is activated and the NMJ during the oxidative stress response.

489           Aldicarb resistance can arise from defects in acetylcholine release from  
490 NMJs, neuropeptide secretion or muscle excitability. We previously found that the  
491 aldicarb resistance caused by SKN-1 activation is not due to enhanced detoxification  
492 of aldicarb or alterations in muscle excitability but instead is due to reduction in  
493 neurotransmitter release from motor neurons (Staab et al., 2013). We subsequently  
494 found that inhibition of intestinal SPHK-1 by SKN-1 results in a reduction in  
495 neuropeptide secretion from motor neurons (Kim and Sieburth, 2018b). Since EGL-  
496 15 is required for the effects of SPHK-1 on NMJ function, we speculate that FGF  
497 signaling may also regulate neuropeptide secretion, although further analysis will be



498 needed to determine the detailed mechanism by which FGFR and IR signaling  
499 regulates NMJ function.

500

### 501 **FGF signaling in regulating NMJ function**

502 Our results are consistent with the idea that EGL-17 activates EGL-15 to  
503 regulate aldicarb response. The *egl-15* gene encodes two receptor isoforms, EGL-  
504 15(A) and EGL-15(B) generated by alternative splicing, that differ in their  
505 extracellular domains and are proposed to have different ligand binding specificity.  
506 EGL-17 binds to EGL-15(A) to mediate migration of sex myoblasts(SM) while LET-  
507 756 binds to EGL-15(B) to regulate development and neuronal growth (Birnbaum et  
508 al., 2005). Because *egl-17* null mutants did not fully block arsenite induced aldicarb  
509 resistance, it is possible that EGL-17 and LET-756 or another unidentified ligand  
510 may function redundantly to regulate aldicarb responsiveness.

511 Our results show that mutations in any single known downstream component  
512 of the EGL-15 pathway attenuate but do not block the arsenite induced aldicarb  
513 resistance, suggesting that there may be signaling redundancy among these  
514 components, or there may be other unidentified EGL-15 effectors. In mammals, the  
515 FGFR activates multiple different cytosolic signaling factors in a signal and context  
516 dependent manner. Additional downstream targets of FGFR that were not tested  
517 here include the adapter proteins FRS2a and CRKL, and well as STAT family  
518 members (Ornitz and Itoh, 2015). It will be interesting to determine whether these  
519 genes function with SOC-1 and/or SOS-1 in this pathway. Interestingly, we found  
520 that in the absence of arsenite, *let-756* or *soc-2* mutants were significantly

521 hypersensitive to aldicarb-induced paralysis, whereas *soc-1* and *sem-5* mutants  
522 were resistant to aldicarb, revealing previously unreported roles for these signaling  
523 components in negatively and positively regulating NMJ function, respectively. The  
524 aldicarb resistance of *sem-5* mutants complicates the interpretation of the relatively  
525 small shift to aldicarb resistance in *sem-5* mutants upon arsenite treatment: it may  
526 reflect a requirement of SEM-5 in promoting arsenite responsiveness, or it could  
527 represent a ceiling effect given the extreme aldicarb resistance of the mutant under  
528 baseline conditions. Further experiments will be needed to determine whether SEM-  
529 5 is involved in this pathway.

530         How does EGL-15 signaling regulate aldicarb responsiveness in response to  
531 stress? EGL-15 has a post-developmental function in regulating fluid homeostasis  
532 (Huang and Stern, 2004). However, defects in fluid homeostasis are not likely to  
533 account for the aldicarb phenotypes of *egl-15* mutants, since *let-756* mutants, which  
534 are also defective in fluid homeostasis, did not block arsenite-induced aldicarb  
535 resistance, whereas *egl-17* mutants, which are not defective in fluid homeostasis,  
536 behaved similarly to *egl-15* mutants. Thus, the aldicarb phenotypes of the FGF  
537 mutants do not correlate with defects in fluid homeostasis. EGL-17 release from the  
538 hypodermis is required for sex myoblast migration during development, and in  
539 adults, EGL-17 is expressed in several cells of the ventral in the hypodermis, as well  
540 as in a pharyngeal neuron (Burdine et al., 1998; Dixon et al., 2006; Hunt-Newbury et  
541 al., 2007). Thus, increased EGL-17 secretion from either of these sites may activate  
542 EGL-15 signaling in the skin in response to stress.

543

## 544 **Insulin-like receptor signaling in regulating NMJ function**

545           Our results suggest that the insulin receptor DAF-2 regulates SKN-1 mediated  
546 NMJ function in response to oxidative stress, and that DAF-2 function is likely  
547 required in multiple tissues. Selective expression of DAF-2 in neurons and muscle  
548 restores hypoxic death to *daf-2* mutants which are highly resistant to hypoxia (Scott  
549 et al., 2002). Neuronal DAF-2 is involved in life span extension and dauer formation  
550 of *daf-2* mutants whereas DAF-2 function in muscle, which is required for fat  
551 metabolism, is not critical for life span extension and dauer phenotype (Wolkow et  
552 al., 2000) suggesting that biological function of DAF-2 is highly tissue-specific. We  
553 speculate that DAF-2 associated NMJ function in response to stress may be  
554 occurring in multiple tissues by inter-tissue signaling mediated by one or more of the  
555 40 insulins in *C. elegans* (Zheng et al., 2018). We showed that DAF-2 functions  
556 independently of DAF-16 to regulate NMJ function. Similarly, DAF-2 functions  
557 independently of DAF-16 in muscles to inhibit protein degradation and promote  
558 proper mobility (Szewczyk et al., 2007). Notably, we found that selective expression  
559 of *daf-2* in the hypodermis led to aldicarb resistance (Figure 5D), a phenotype that  
560 was not observed when expressing *daf-2* in any other tissue tested, suggesting that  
561 enhanced DAF-2 signaling in the hypodermis may regulate NMJ function in the  
562 absence of stress. Indeed, DAF-2 signaling has been implicated in decreasing motor  
563 function in aged animals, but its site of action was not determined (Liu et al., 2013).

564           Our results suggest that DAF-2 signaling functions downstream of SKN-1 to  
565 regulate NMJ function. Consistent with this, tyrosine phosphorylation of the insulin  
566 receptor substrates 1 and 2 (IRS-1 and -2) by the insulin receptor is strongly reduced  
567 in the Nrf2-deficient mice (Beyer and Werner, 2008). Furthermore, insulin receptor

568 tyrosine kinase is greatly activated by oxidative stressor hydrogen peroxide (Droge,  
569 2005). Interestingly, DAF-2 signaling has been implicated in the activation of SKN-1  
570 during aging through the regulation of the Akt kinases AKT-1/2 (Tullet et al., 2008).  
571 The function of DAF-2 downstream of SKN-1 that we report here is likely to be  
572 distinct from the function identified for DAF-2 during ageing, further underscoring the  
573 complex role of insulin signaling in the SKN-1 pathway.

574

### 575 **Acknowledgements**

576 We thank members of the lab for advice and critical review of the manuscript, and  
577 Mei Zhen for providing DAF-2 plasmids. This work was supported by grants from the  
578 NIH National Institute of Neurological Disorders and Stroke (NINDS) to D.S.  
579 (NS071085 and NS099414). Some strains were provided by the Caenorhabditis  
580 Genetics Center (CGC), which is funded by the NIH Office of Research Infrastructure  
581 Programs (P40 OD010440).

582

### 583 **References**

584

585 Abdus-Saboor, I., Mancuso, V.P., Murray, J.I., Palozola, K., Norris, C., Hall, D.H., Howell, K.,  
586 Huang, K., and Sundaram, M.V. (2011). Notch and Ras promote sequential steps of  
587 excretory tube development in *C. elegans*. *Development* *138*, 3545-3555.  
588 Beyer, T.A., and Werner, S. (2008). The cytoprotective Nrf2 transcription factor controls  
589 insulin receptor signaling in the regenerating liver. *Cell Cycle* *7*, 874-878.  
590 Birnbaum, D., Popovici, C., and Roubin, R. (2005). A pair as a minimum: the two fibroblast  
591 growth factors of the nematode *Caenorhabditis elegans*. *Dev Dyn* *232*, 247-255.  
592 Blackwell, T.K., Steinbaugh, M.J., Hourihan, J.M., Ewald, C.Y., and Isik, M. (2015). SKN-  
593 1/Nrf, stress responses, and aging in *Caenorhabditis elegans*. *Free Radic Biol Med* *88*,  
594 290-301.

- 595 Bulger, D.A., Fukushige, T., Yun, S., Semple, R.K., Hanover, J.A., and Krause, M.W. (2017).  
596 *Caenorhabditis elegans* DAF-2 as a Model for Human Insulin Receptoropathies. *G3* *7*,  
597 257-268.
- 598 Bulow, H.E., Boulin, T., and Hobert, O. (2004). Differential functions of the *C. elegans* FGF  
599 receptor in axon outgrowth and maintenance of axon position. *Neuron* *42*, 367-374.
- 600 Burdine, R.D., Branda, C.S., and Stern, M.J. (1998). EGL-17(FGF) expression coordinates the  
601 attraction of the migrating sex myoblasts with vulval induction in *C. elegans*.  
602 *Development* *125*, 1083-1093.
- 603 Burdine, R.D., Chen, E.B., Kwok, S.F., and Stern, M.J. (1997). *egl-17* encodes an  
604 invertebrate fibroblast growth factor family member required specifically for sex myoblast  
605 migration in *Caenorhabditis elegans*. *Proc Natl Acad Sci U S A* *94*, 2433-2437.
- 606 Chan, J.P., Hu, Z., and Sieburth, D. (2012). Recruitment of sphingosine kinase to  
607 presynaptic terminals by a conserved muscarinic signaling pathway promotes  
608 neurotransmitter release. *Genes Dev* *26*, 1070-1085.
- 609 Chen, D., Li, P.W., Goldstein, B.A., Cai, W., Thomas, E.L., Chen, F., Hubbard, A.E., Melov, S.,  
610 and Kapahi, P. (2013). Germline signaling mediates the synergistically prolonged  
611 longevity produced by double mutations in *daf-2* and *rks-1* in *C. elegans*. *Cell reports* *5*,  
612 1600-1610.
- 613 Choe, K.P., Przybysz, A.J., and Strange, K. (2009). The WD40 repeat protein WDR-23  
614 functions with the CUL4/DDB1 ubiquitin ligase to regulate nuclear abundance and  
615 activity of SKN-1 in *Caenorhabditis elegans*. *Mol Cell Biol* *29*, 2704-2715.
- 616 DeVore, D.L., Horvitz, H.R., and Stern, M.J. (1995). An FGF receptor signaling pathway is  
617 required for the normal cell migrations of the sex myoblasts in *C. elegans*  
618 hermaphrodites. *Cell* *83*, 611-620.
- 619 Diaz-Balzac, C.A., Lazaro-Pena, M.I., Ramos-Ortiz, G.A., and Bulow, H.E. (2015). The  
620 Adhesion Molecule KAL-1/anosmin-1 Regulates Neurite Branching through a SAX-  
621 7/L1CAM-EGL-15/FGFR Receptor Complex. *Cell reports* *11*, 1377-1384.
- 622 Dixon, S.J., Alexander, M., Fernandes, R., Ricker, N., and Roy, P.J. (2006). FGF negatively  
623 regulates muscle membrane extension in *Caenorhabditis elegans*. *Development* *133*,  
624 1263-1275.
- 625 Droge, W. (2005). Oxidative stress and ageing: is ageing a cysteine deficiency syndrome?  
626 *Philosophical transactions of the Royal Society of London Series B, Biological sciences*  
627 *360*, 2355-2372.
- 628 Duhon, S.A., and Johnson, T.E. (1995). Movement as an index of vitality: comparing wild  
629 type and the *age-1* mutant of *Caenorhabditis elegans*. *J Gerontol A Biol Sci Med Sci* *50*,

630 B254-261.

631 Gottlieb, S., and Ruvkun, G. (1994). *daf-2*, *daf-16* and *daf-23*: genetically interacting genes  
632 controlling Dauer formation in *Caenorhabditis elegans*. *Genetics* *137*, 107-120.

633 Hsu, A.L., Feng, Z., Hsieh, M.Y., and Xu, X.Z. (2009). Identification by machine vision of the  
634 rate of motor activity decline as a lifespan predictor in *C. elegans*. *Neurobiol Aging* *30*,  
635 1498-1503.

636 Huang, P., and Stern, M.J. (2004). FGF signaling functions in the hypodermis to regulate  
637 fluid balance in *C. elegans*. *Development* *131*, 2595-2604.

638 Hung, W.L., Wang, Y., Chitturi, J., and Zhen, M. (2014). A *Caenorhabditis elegans*  
639 developmental decision requires insulin signaling-mediated neuron-intestine  
640 communication. *Development* *141*, 1767-1779.

641 Hunt-Newbury, R., Viveiros, R., Johnsen, R., Mah, A., Anastas, D., Fang, L., Halfnight, E.,  
642 Lee, D., Lin, J., Lorch, A., *et al.* (2007). High-throughput in vivo analysis of gene expression  
643 in *Caenorhabditis elegans*. *PLoS Biol* *5*, e237.

644 Inoue, H., Hisamoto, N., An, J.H., Oliveira, R.P., Nishida, E., Blackwell, T.K., and Matsumoto,  
645 K. (2005). The *C. elegans* p38 MAPK pathway regulates nuclear localization of the  
646 transcription factor SKN-1 in oxidative stress response. *Genes Dev* *19*, 2278-2283.

647 Kamath, R.S., and Ahringer, J. (2003). Genome-wide RNAi screening in *Caenorhabditis*  
648 *elegans*. *Methods* *30*, 313-321.

649 Kauffman, A.L., Ashraf, J.M., Corces-Zimmerman, M.R., Landis, J.N., and Murphy, C.T.  
650 (2010). Insulin signaling and dietary restriction differentially influence the decline of  
651 learning and memory with age. *PLoS Biol* *8*, e1000372.

652 Kim, K.W., and Jin, Y. (2015). Neuronal responses to stress and injury in *C. elegans*. *FEBS*  
653 *Lett* *589*, 1644-1652.

654 Kim, S., and Sieburth, D. (2018a). Sphingosine Kinase Activates the Mitochondrial  
655 Unfolded Protein Response and Is Targeted to Mitochondria by Stress. *Cell reports* *24*,  
656 2932-2945 e2934.

657 Kim, S., and Sieburth, D. (2018b). Sphingosine Kinase Regulates Neuropeptide Secretion  
658 During the Oxidative Stress-Response Through Intertissue Signaling. *J Neurosci* *38*, 8160-  
659 8176.

660 Leung, C.K., Hasegawa, K., Wang, Y., Deonaraine, A., Tang, L., Miwa, J., and Choe, K.P.  
661 (2014). Direct interaction between the WD40 repeat protein WDR-23 and SKN-1/Nrf  
662 inhibits binding to target DNA. *Mol Cell Biol* *34*, 3156-3167.

663 Li, L.B., Lei, H., Arey, R.N., Li, P., Liu, J., Murphy, C.T., Xu, X.Z., and Shen, K. (2016). The  
664 Neuronal Kinesin UNC-104/KIF1A Is a Key Regulator of Synaptic Aging and Insulin

- 665 Signaling-Regulated Memory. *Curr Biol* *26*, 605-615.
- 666 Libina, N., Berman, J.R., and Kenyon, C. (2003). Tissue-specific activities of C-elegans DAF-  
667 16 in the regulation of lifespan. *Cell* *115*, 489-502.
- 668 Liu, J., Zhang, B., Lei, H., Feng, Z., Liu, J., Hsu, A.L., and Xu, X.Z. (2013). Functional aging in  
669 the nervous system contributes to age-dependent motor activity decline in *C. elegans*.  
670 *Cell Metab* *18*, 392-402.
- 671 Lo, T.W., Branda, C.S., Huang, P., Sasson, I.E., Goodman, S.J., and Stern, M.J. (2008).  
672 Different isoforms of the *C. elegans* FGF receptor are required for attraction and  
673 repulsion of the migrating sex myoblasts. *Dev Biol* *318*, 268-275.
- 674 McKay, S.J., Johnsen, R., Khattra, J., Asano, J., Baillie, D.L., Chan, S., Dube, N., Fang, L.,  
675 Goszczynski, B., Ha, E., *et al.* (2003). Gene expression profiling of cells, tissues, and  
676 developmental stages of the nematode *C. elegans*. *Cold Spring Harb Symp Quant Biol*  
677 *68*, 159-169.
- 678 Mello, C.C., Kramer, J.M., Stinchcomb, D., and Ambros, V. (1991). Efficient gene transfer in  
679 *C.elegans*: extrachromosomal maintenance and integration of transforming sequences.  
680 *Embo J* *10*, 3959-3970.
- 681 Mounsey, A., Bauer, P., and Hope, I.A. (2002). Evidence suggesting that a fifth of  
682 annotated *Caenorhabditis elegans* genes may be pseudogenes. *Genome Res* *12*, 770-775.
- 683 Murakami, H., Bessinger, K., Hellmann, J., and Murakami, S. (2005). Aging-dependent and  
684 -independent modulation of associative learning behavior by insulin/insulin-like growth  
685 factor-1 signal in *Caenorhabditis elegans*. *J Neurosci* *25*, 10894-10904.
- 686 Olofsson, B. (2014). The olfactory neuron AWC promotes avoidance of normally palatable  
687 food following chronic dietary restriction. *The Journal of experimental biology* *217*, 1790-  
688 1798.
- 689 Ornitz, D.M., and Itoh, N. (2015). The Fibroblast Growth Factor signaling pathway. *Wiley*  
690 *interdisciplinary reviews Developmental biology* *4*, 215-266.
- 691 Paek, J., Lo, J.Y., Narasimhan, S.D., Nguyen, T.N., Glover-Cutter, K., Robida-Stubbs, S.,  
692 Suzuki, T., Yamamoto, M., Blackwell, T.K., and Curran, S.P. (2012). Mitochondrial SKN-  
693 1/Nrf mediates a conserved starvation response. *Cell Metab* *16*, 526-537.
- 694 Popovici, C., Conchonaud, F., Birnbaum, D., and Roubin, R. (2004). Functional phylogeny  
695 relates LET-756 to fibroblast growth factor 9. *J Biol Chem* *279*, 40146-40152.
- 696 Popovici, C., Roubin, R., Coulier, F., Pontarotti, P., and Birnbaum, D. (1999). The family of  
697 *Caenorhabditis elegans* tyrosine kinase receptors: similarities and differences with  
698 mammalian receptors. *Genome Res* *9*, 1026-1039.
- 699 Schutzman, J.L., Borland, C.Z., Newman, J.C., Robinson, M.K., Kokel, M., and Stern, M.J.

700 (2001). The *Caenorhabditis elegans* EGL-15 signaling pathway implicates a DOS-like  
701 multisubstrate adaptor protein in fibroblast growth factor signal transduction. *Mol Cell*  
702 *Biol* *21*, 8104-8116.

703 Scott, B.A., Avidan, M.S., and Crowder, C.M. (2002). Regulation of hypoxic death in *C.*  
704 *elegans* by the insulin/IGF receptor homolog DAF-2. *Science* *296*, 2388-2391.

705 Simon, M., Sarkies, P., Ikegami, K., Doebley, A.L., Goldstein, L.D., Mitchell, J., Sakaguchi, A.,  
706 Miska, E.A., and Ahmed, S. (2014). Reduced insulin/IGF-1 signaling restores germ cell  
707 immortality to *Caenorhabditis elegans* Piwi mutants. *Cell reports* *7*, 762-773.

708 Staab, T.A., Griffen, T.C., Corcoran, C., Evgrafov, O., Knowles, J.A., and Sieburth, D. (2013).  
709 The conserved SKN-1/Nrf2 stress response pathway regulates synaptic function in  
710 *Caenorhabditis elegans*. *PLoS Genet* *9*, e1003354.

711 Sun, X., Chen, W.D., and Wang, Y.D. (2017). DAF-16/FOXO Transcription Factor in Aging  
712 and Longevity. *Frontiers in pharmacology* *8*, 548.

713 Sundaram, M., Yochem, J., and Han, M. (1996). A Ras-mediated signal transduction  
714 pathway is involved in the control of sex myoblast migration in *Caenorhabditis elegans*.  
715 *Development* *122*, 2823-2833.

716 Szewczyk, N.J., and Jacobson, L.A. (2003). Activated EGL-15 FGF receptor promotes  
717 protein degradation in muscles of *Caenorhabditis elegans*. *EMBO J* *22*, 5058-5067.

718 Szewczyk, N.J., Peterson, B.K., Barmada, S.J., Parkinson, L.P., and Jacobson, L.A. (2007).  
719 Opposed growth factor signals control protein degradation in muscles of *Caenorhabditis*  
720 *elegans*. *EMBO J* *26*, 935-943.

721 Tullet, J.M., Hertweck, M., An, J.H., Baker, J., Hwang, J.Y., Liu, S., Oliveira, R.P., Baumeister,  
722 R., and Blackwell, T.K. (2008). Direct inhibition of the longevity-promoting factor SKN-1  
723 by insulin-like signaling in *C. elegans*. *Cell* *132*, 1025-1038.

724 Wolkow, C.A., Kimura, K.D., Lee, M.S., and Ruvkun, G. (2000). Regulation of *C. elegans* life-  
725 span by insulinlike signaling in the nervous system. *Science* *290*, 147-150.

726 Wu, C.W., Deonaraine, A., Przybysz, A., Strange, K., and Choe, K.P. (2016). The Skp1  
727 Homologs SKR-1/2 Are Required for the *Caenorhabditis elegans* SKN-1  
728 Antioxidant/Detoxification Response Independently of p38 MAPK. *PLoS Genet* *12*,  
729 e1006361.

730 Zheng, S., Chiu, H., Boudreau, J., Papanicolaou, T., Bendena, W., and Chin-Sang, I. (2018).  
731 A functional study of all 40 *Caenorhabditis elegans* insulin-like peptides. *The Journal of*  
732 *biological chemistry* *293*, 16912-16922.

733